A Thesis

for the Degree of Master of Science in Medicine

Photoprotective Activity of Isorhamnetin in UVB-Damaged Human HaCaT Keratinocytes

Graduate School, Jeju National University

Department of Medicine

Xia Han

February, 2016

자외선 B에 의해 손상된 인간 HaCaT 각질형성세포에서 isorhamnetin의 광 보호 활성

지도교수 현 진 원

한 하

이 논문을 의학 석사학위 논문으로 제출함

2015년 12월

한하의 의학 석사학위 논문을 인준함

심사위원장 ..... 차德喜

위 원 ..... 강희정

위 원 ..... 현진원

제주대학교 대학원

2015년 12월

Photoprotective Activity of Isorhamnetin in UVB-Damaged Human HaCaT Keratinocytes

Xia Han

(Supervised by professor Jin Won Hyun)

A thesis submitted for the partial fulfillment of the requirement for the degree of Master of Science in Medicine

December, 2015

This thesis has been examined and approved.

Deok Bae Park

Heelyoung Kang

Jin Won Hyun

2015. 12. 16

Date

Department of Medicine

GRADUATE SCHOOL

JEJU NATIONAL UNIVERSITY

ABSTRACT

The purpose of this study was to characterize the photoprotective properties of isorhamnetin (3-methylquercetin), an isolated flavonoid from certain medicinal plants, against cell injury and damage in human HaCaT keratinocytes resulting from ultraviolet (UV) B exposure. Isorhamnetin exhibited scavenging capacity of UVB-generated intracellular reactive oxygen species and repressed UVB-facilitated apoptosis in the human HaCaT keratinocyte, as evidenced by decreasing apoptotic body formation, nuclear fragmentation, and apoptotic sub-G1 DNA fraction. Furthermore, isorhamnetin attenuated the oxidative related macromolecular damage of lipids, proteins, and DNA in response to UVB radiation. In addition, isorhamnetin salved HaCaT cells from UVB light triggered mitochondrial dysfunction. Taken together, these findings implied that isorhamnetin has the peculiarity to be developed as an efficient agent against UVB-mediated skin disease.

CONTENTS

LIST OF FIGURES

1. Introduction

Excessive or chronic ultraviolet (UV) radiation induces many types of skin damage, including sunburn, photoaging, corneal injury, and inflammation; extreme UV exposure can even jeopardize the immune system (Matsumura and Ananthaswamy, 2004; Liu *et al*., 2012). UV radiation consists of three kinds of energy: UVA (~320–540 nm), UVB (~280–320 nm), and UVC (~100–320 nm) light. While UVA and UVB light both can provoke skin damage, the latter is approximately 1000 times stronger than the former and accordingly, is associated with graver biological insults.

UVB radiation is mostly absorbed in the epidermis skin layer where most skin cancers occur. UVB radiation is mainly affects epidermal cells, especially keratinocytes which are the predominant cell population in skin epidermis layer, and these cells are the primary targets of UVB (Zeng *et al*., 2014). However, ~10–30% of UVB energy can reach the upper dermis, and hence, UVB light is also hazard to fibroblasts and the extracellular matrix (Rosette and Karin, 1996; Everett *et al*., 1966). Additionally, UVB light interacts with intracellular chromophores and photosensitizers to engender severe oxidative stress in skin cells, together with transient as well as permanent genetic damage. At a more fundamental level, these oxidative reactions activate cytoplasmic signal transduction pathways which are associated with cell growth, differentiation, and senescence, and ultimately, connective tissue degradation (Helenius *et al*., 1999).

UVB radiation triggers two predominant types of cytotoxic damage to the skin that interfere with normal cellular functions, and finally culminate in photodamage, photoaging, and photocarcinogenesis (Sander *et al*., 2004). In the first type, UVB light directly and efficiently absorbed by DNA causes the development of DNA damage in the form of cyclobutane pyrimidine dimers and 6-4 photoproducts (Budden and Bowden, 2013). The second type is UVB light indirectly damages DNA, lipids, membranes, and proteins via generation of unwarranted levels of reactive oxygen species (ROS) (Wäster and Ollinger, 2009; Lee *et al*., 2013). Although our skin has efficient antioxidant defense mechanisms against a variety

of endogenous and exogenous insults (Lyu and Park, 2012), an overabundance of UVB-induced ROS disrupts this defensive capacity and precipitates irrevocable oxidative injury (Scandalios, 2002).

Natural antioxidants have received ample attention as prospective preventative or curative agents against skin disease and damage caused by long-term or extreme exposure to UVB (Afaq 2011; Yin *et al*., 2013). For example, isorhamnetin is an antioxidant flavonoid derived from the fruits of certain medicinal plants, including *Hippophae rhamnoides* L., also known as common sea buckthorn (Li *et al*., 2014; Yang *et al*., 2014). Nevertheless, the photoprotective role of isorhamnetin against UVB-provoked skin damage remains unknown. Accordingly, this study examined the ability of isorhamnetin to safeguard cultured human keratinocytes from injury resulting from UVB exposure.

2. Materials and Methods

2-1. Reagents

Isorhamnetin (3,5,7-trihydroxy-2-(4-hydroxy-3-methoxyphenyl)-4-benzopyrone, purity: ≥98%) was purchased from Santa Cruz Biotechnology Co. (Santa Cruz, CA, USA) and dissolved in dimethylsulfoxide (DMSO) (with ultimate density not exceed 0.02% in further experiments). MTT (3-(4,5-dimethylthiazol-2-yl)-2,5-diphenyltetrazolium bromide), DMPO (5,5-dimethyl-1-pyrroline-N-oxide), NAC (N-acetyl cysteine), DCF-DA (2′,7′-dichlorofluorescin diacetate) and Hoechst 33342 dye were purchased from Sigma Chemical Co. (St. Louis, MO, USA). While 5,5′,6,6′-tetrachloro-1,1′,3,3′-tetraethyl-benzimidazolylcarbocyanine iodide (JC-1 dye) was purchased from Invitrogen (Carlsbad, CA, USA), and diphenyl-1-pyrenylphosphine (DPPP) was bought from Molecular Probes (Eugene, OR, USA). All other chemicals and reagents were of analytical grade.

2-2. Electron spin resonance (ESR) spectrometry for superoxide anion and hydroxyl radical detection

The superoxide anion was generated from xanthine/xanthine oxidase system can react with the nitrone spin trap, DMPO. The resultant DMPO/•OOH adducts were detected by a JES-FA ESR spectrometer (JEOL, Ltd., Tokyo, Japan), as previously described (Ueno *et al*., 1984; Kohno *et al*., 1994). Briefly, isorhamnetin (20 μL; 5 μM) was mixed with xanthine oxidase (0.25 U), xanthine (10 mM), and DMPO (3 M), and then ESR signaling was recorded at 2.5 min after reaction occurrence. The ESR spectrometry parameters were set as follows: center field = 336 mT, power = 1.00 mW, modulation width = 0.2 mT, sweep time = 30 sec, sweep width = 10 mT, time constant = 0.03 sec, and temperature = 25 ℃.

Next, the Fenton reaction (H_2O_2 + $FeSO_4$) was employed to generate the hydroxyl radical, and the generated hydroxyl radical was reacted with DMPO. The resultant DMPO/•OH adducts were detected using an ESR spectrometer, as previously described (Li *et al*., 2003). The ESR spectrum was recorded at

2.5 min after isorhamnetin (20 μL; 5 μM) was mixed with $FeSO_4$ (10 mM), H_2O_2 (10 mM), and DMPO (0.3 M). The ESR spectrometry parameters were set as indicated above for superoxide anion detection.

2-3. Cell culture

The human keratinocyte HaCaT cell line was supplied by Amore Pacific Co. (Gyeonggi-do, Korea). Cells were incubated in a 5% CO_2/95% atmosphere at 37℃ in RPMI 1640 medium (Invitrogen, Grand Island, NY, USA) containing 10% heat-inactivated fetal calf serum (heated at 56℃ for 45 min), streptomycin (100 μg/mL), and penicillin (100 units/mL).

2-4. Cell viability assay

The potential cytotoxicity of isorhamnetin against HaCaT keratinocytes was investigated by the colorimetric MTT assay, which is based on the reduction of a tetrazolium salt to purple formazan by mitochondrial dehydrogenases in viable cells. The purple formazan can be dissolved in DMSO then quantified by measuring at a specific wavelength. Cells were seeded into 24-well plates at a density of 1.0 $\times 10^5$ cells/mL. Sixteen hours later, they were pretreated with isorhamnetin at concentrations of 0, 2.5, 5, 10, and 20 μM.

The photoprotective actions of isorhamnetin against UVB radiation were next assessed in HaCaT keratinocytes. Cells were pretreated with isorhamnetin (5 μM) for 1 h, subjected to UVB exposure at a dose of 30 mJ/cm^2, and then incubated at 37℃ for additional 24 h. MTT stock solution (50 μL; 2 mg/mL) was added to each well to yield a total reaction volume of 200 μL. After incubation for 4 h, the medium was aspirated. The formazan crystals in each well were dissolved in DMSO (150 μL), and the absorbance at 540 nm was read on a scanning multi-well spectrophotometer (Carmichael *et al*., 1987).

2-5. Measurement of intracellular ROS

To measure intracellular ROS contents in UVB-irradiated HaCaT keratinocytes, cells were seeded into 24-well plates at a density of 1.0 $\times 10^5$ cells/mL. Sixteen hours later, the cells were pretreated for 1 h at

37℃ with 5 μM isorhamnetin and 1 mM NAC, a powerful antioxidant used as positive control, respectively. Next, the cells were exposed to UVB radiation (30 mJ/cm^2). 24 hours later, the cells were loaded with DCF-DA solution (50 μM) and incubated for 30 min at 37℃. The fluorescence of the 2′,7′-dichlorofluorescein (DCF) product was detected and quantitated using a LS-5B spectrofluorometer (PerkinElmer, Waltham, MA, USA).

Additionally, the ROS scavenging potential of isorhamnetin was evaluated in UVB-irradiated cells via flow cytometry. Cells were seeded into 60-mm dish at a density of 1.0 × 10^5 cells/mL. Sixteen hours after plating, they were pretreated with 5 μM isorhamnetin for 1 h, exposed to UVB light (30 mJ/cm^2), and incubated for an additional 9 h at 37℃. Cells were then loaded with DCF-DA (40 μM) and incubated for 30 min at 37℃. The fluorescence of the DCF product was detected via flow cytometry by a FACSCalibur instrument (Becton Dickinson, Mountain View, CA, USA) (Rosenkranz *et al*., 1992).

Lastly, image analysis of intracellular ROS was conducted by seeding the keratinocytes onto four-well chamber slides at a density of 1.0 × 10^5 cells/mL. Sixteen hours after plating, the cells were pretreated with 5 μM isorhamnetin for 1 h, and then irradiated with UVB light (30 mJ/cm^2). After an additional 24 h, 40 μM DCF-DA were added to each well, and the samples were incubated for another 30 min at 37℃. The stained cells were then washed with PBS and mounted onto a chamber slide in mounting medium (Dako, Carpentaria, CA, USA). Images of the cultures were captured by an LSM 5 PASCAL laser scanning confocal microscope and the accompanying LSM 5 PASCAL software (Carl Zeiss, Jena, Germany).

2-6. Nucleus staining with Hoechst 33342 dye

HaCaT keratinocytes were separately pretreated with 5 μM isorhamnetin and 1 mM NAC for 1 h, followed by exposure to UVB light (30 mJ/cm^2). After an additional incubation for 24 h at 37℃, each well was loaded with a DNA-specific fluorescent dye, Hoechst 33342 (20 μM), subsequently incubated for another 10 min at 37℃. The stained cells were captured using a fluorescence microscope equipped with a CoolSNAP-Pro color digital camera. The apoptotic cells were counted, and the degree of nuclear

condensation was evaluated.

2-7. Determination of mitochondrial membrane potential ($\Delta\psi_m$)

HaCaT cells were seeded into 60-mm dish at a density of 1.0×10^5 cells/mL. after 16 hours plating, the cells were pretreated with 5 μM isorhamnetin for 1 h, exposed to UVB radiation (30 mJ/cm^2), and then incubated for an additional 24 h at 37℃. The $\Delta\psi_m$ was analyzed using MitoPT™ JC-1 reagent, a lipophilic cationic fluorescent dye that easily penetrates cell and mitochondrial lipid bilayer membrane barriers. When the mitochondrial membrane potential collapses in apoptotic or metabolically stressed cells, JC-1 disperses throughout the cell in monomeric form and emits green fluorescence upon excitation at 488 nm. After addition of 5 μM JC-1 and incubation for 30 min at 37℃ (Cossarizza *et al*., 1993), images of the cultures were captured by an LSM 5 PASCAL laser scanning confocal microscope and the accompanying LSM 5 PASCAL software (Carl Zeiss, Jena, Germany), and the $\Delta\psi_m$ was also analyzed in HaCaT keratinocytes via flow cytometry by a FACSCalibur instrument.

2-8. Detection of sub-G1 hypodiploid cells

Cells were pretreated with 5 μM isorhamnetin for 1 h, and subjected to UVB radiation (30 mJ/cm^2) for 24 h incubation. Afterwards, 70% ethanol (1 mL) was used to make the cells easy to incorporation of propidium iodide (PI) for 30 min at room temperature. The cells were washed twice with PBS-2 mM EDTA (prevention of cell aggregation) and incubated in the dark for 30 min at 37℃ in PBS-2 mM EDTA containing RNase A (final 100 μg/mL) and PI (final 100 μg/mL). Flow cytometric analysis was performed by a FACSCalibur instrument. The sub-G1 hypodiploid cells was measured based on histograms generated by CellQuest and ModFit Software (Becton Dickinson). Staining-based flow cytometry was performed to evaluate the of apoptotic sub-G1 fraction cells with hypodiploid DNA contents.

2-9. Terminal deoxynucleotidyl transferase-mediated digoxigenin-dUTP nick end labeling (TUNEL) assay

The TUNEL assay allows the detection of DNA fragmentation by labeling the terminal end of nucleic acids, which was performed using an in situ cell death detection kit (Roche Diagnostics, Mannheim, Germany). Briefly, HaCaT keratinocytes were seeded onto chamber slides at a density of 1.0×10^5 cells/mL. Sixteen hours later, the cells were pretreated with isorhamnetin (5 μM) for 1 h and then radiated with UVB (30 mJ/cm^2). After an additional 24 h incubation, cells were fixed with 4% paraformaldehyde for 30 min at room temperature, permeated with 0.2% Triton X-100 for 2 min, washed twice with PBS, and incubated with the TUNEL reaction mixture for 1 h at 37℃. Finally, the stained cells were washed with PBS and mounted onto a microscope slide in mounting medium. Images of the cells were captured and quantified by an Olympus IX 70 fluorescence microscope (Olympus Optical Co., Tokyo, Japan).

2-10. Single-cell gel electrophoresis (comet assay)

Oxidative DNA strand breakage was detected via the comet assay, also known as single-cell gel electrophoresis (Rajagopalan *et al*., 2003; Singh, 2000). Twelve hours after isorhamnetin pretreatment and UVB radiation (30 mJ/cm^2), a suspension of HaCaT keratinocytes was mixed with 75 μL of 0.5% low melting temperature agarose at 39℃, then spread the mixture on a fully frosted microscopic slide pre-coated with 200 μL of 1% normal melting temperature agarose. After the agarose was solidified, then covered the slide with another 75 μL of 0.5% low melting temperature agarose, followed immersing in a lysis solution (2.5 M NaCl, 100 mM Na-EDTA, 10 mM Tris, 1% Trion X-100, and 10% DMSO, pH 10) at 4℃ for 90 min. Next then, placed the slides in a gel electrophoresis apparatus which contains 300 mM NaOH and 10 mM Na-EDTA, pH 13 for 40 min. This step was to allow for DNA unwinding and the expression of alkali-labile damage. The applied electrical field was 300 mA, 25 V for 20 min to draw the negatively charged DNA towards the anode. After washing 3 times with a neutralizing buffer (0.4 M Tris, pH 7.5) for 5 min at 4℃, the slides were loaded with 40 μL of ethidium bromide and visualized by a

fluorescence microscope equipped with a Komet 5.5 image analyzing system (Kinetic Imaging, Ltd., Nottingham, UK). 50 cells per slide were selected to record about the percentages of total cellular fluorescence in the comet tails and the tail lengths.

2-11. Lipid peroxidation assay

Oxidation damage to lipids was assessed by measuring levels of 8-isoprostane, an indicator of lipid peroxidation, secreted into the conditioned medium of irradiated HaCaT keratinocytes via colorimetric determination (Beauchamp *et al*., 2002). A commercial enzyme-linked immunosorbent assay kit (Cayman Chemical, Ann Arbor, MI, USA) was used to detect 8-isoprostane. Lipid peroxidation was also detected using DPPP as a probe (Okimoto *et al*., 2000). Lipid hydroperoxides can oxidize DPPP to DPPP oxide, which is a yield fluorescent product providing as an indication of oxidative membrane damage. The cells were pretreated with 5 μM isorhamnetin for 1 h, followed by UVB radiation (30 mJ/cm^2). Six hours later, incubated the cells with 20 μM DPPP for 30 min in the dark. Images of DPPP oxide fluorescence were visualized under a Zeiss Axiovert 200 inverted microscope with the excitation wavelength of 351 nm and the emission wavelength of 380 nm.

2-12. Protein carbonyl formation

After 1 h of 5 μM isorhamnetin pretreatment, cells were exposed to UVB radiation (30 mJ/cm^2) and incubated for another 24 h. The extent of protein carbonyl formation was determined using an OxiselectTM protein carbonyl enzyme-linked immunosorbent assay kit (Cell Biolabs, San Diego, CA, USA) according to the manufacturer's instructions.

2-13. Statistical analysis

All measurements were performed in triplicate and expressed as the means ± the standard error of the mean. The variance (ANOVA) and Tukey's post-hoc test were subjected to analyze differences between means. In each case, a p value of < 0.05 was considered statistically significant.

3. Results

3-1. Isorhamnetin exhibits capacity of free radicals scavenging in cell-free system and attenuates UVB-generated ROS in HaCaT keratinocytes

The cytotoxicity of isorhamnetin to human HaCaT keratinocytes was performed by a MTT assay. Isorhamnetin itself exerted no cytotoxic actions on the keratinocytes up to concentrations of 5 μM. Nevertheless, a strong cytotoxicity was shown at 10 or 20 μM (Fig. 1A). Therefore, 5 μM isorhamnetin was chosen as the optimal concentration for further experimentation.

Next, the UVB-induced intracellular ROS levels in HaCaT keratinocytes were measured by the oxidation-sensitive fluorescent dye DCF-DA. UVB-irradiated cells showed significantly higher ROS contents compared to untreated control cells. Whereas, isorhamnetin obviously decreased ROS levels in UVB-irradiated cells, as nearly efficacious as NAC, a well-known ROS scavenger used as positive control (Fig. 1B). Subsequently, the results were confirmed by performing flow cytometry after DCF-DA staining to assess the ROS scavenging capacity of isorhamnetin in UVB-irradiated cells. The fluorescence intensity in isorhamnetin-pretreated cells (101) was similar to untreated control (106), signifying that isorhamnetin alone does not generate intracellular ROS. While, the compound substantially attenuated UVB accumulated intracellular ROS (fluorescence intensity 144 vs. 119 for UVB-irradiated vs. UVB-/ isorhamnetin-treated cells, respectively; Fig. 1C). Moreover, the pictorial images of ROS fluorescence captured by confocal microscopy showed consistently findings in flow cytometry (Fig. 1D). Taken together, these results (Fig. 1B–D) indicate that isorhamnetin attenuates UVB-generated ROS in HaCaT keratinocytes.

The scavenging properties of isorhamnetin against the superoxide anion and the hydroxyl radical were also investigated in the cell-free systems by ESR spectrometry. The xanthine/xanthine oxidase system can significantly generate superoxide anion (signal value 2198) compared to untreated control (signal value 162) and isorhamnetin itself (signal value 136). However, the addition of isorhamnetin to the

xanthine/xanthine oxidase system significantly decreased the superoxide anion signal value to 1123 (Fig. 1E). Similar results were found in the Fenton reaction system, where the hydroxyl radical signal value increased from 38 in the control sample and 34 in the isorhamnetin itself to 2170 in the experimental sample, but the addition of isorhamnetin to the experimental sample significantly decreased the hydroxyl radical signal value to 1724 (Fig. 1F).

A

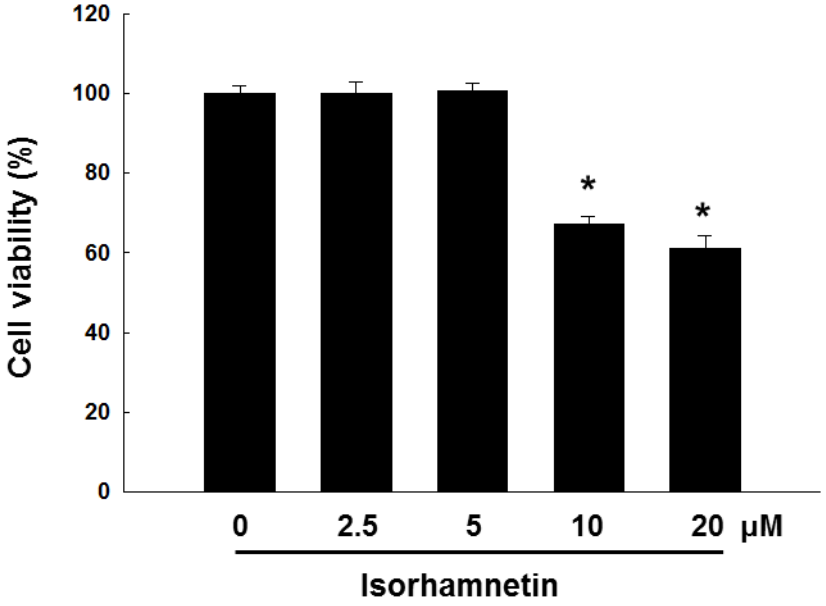

B

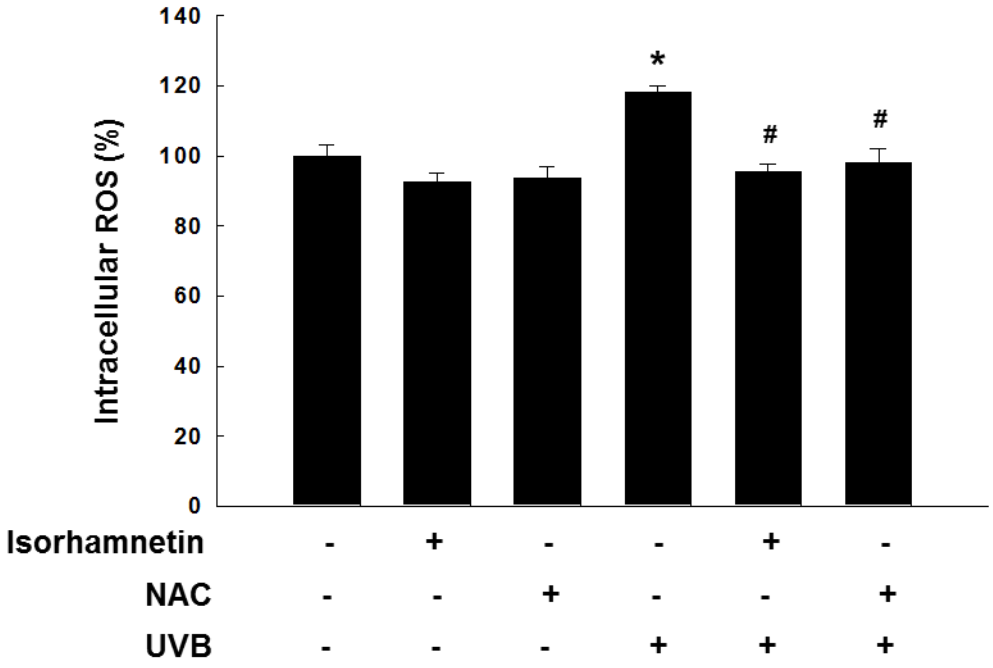

C

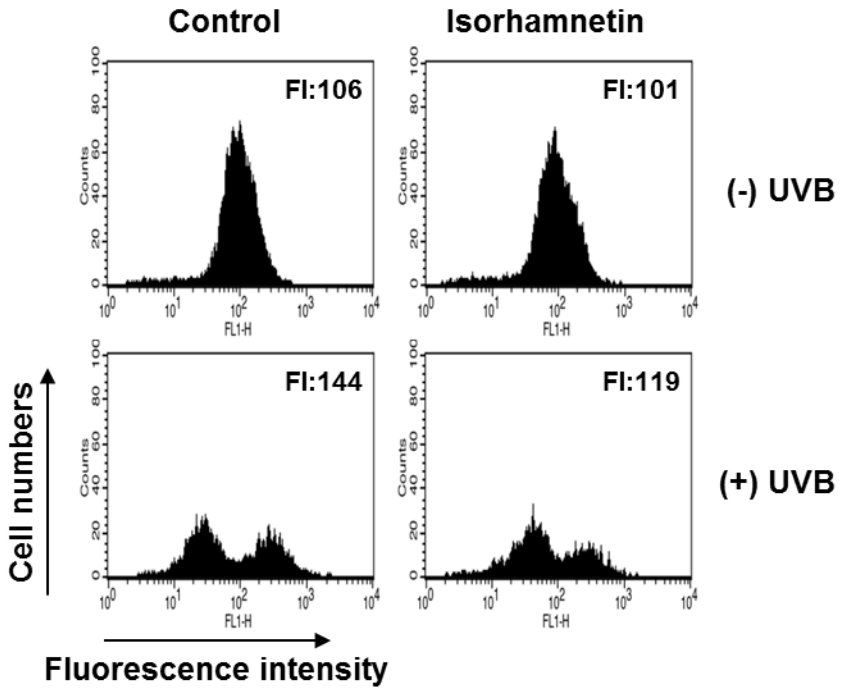

D

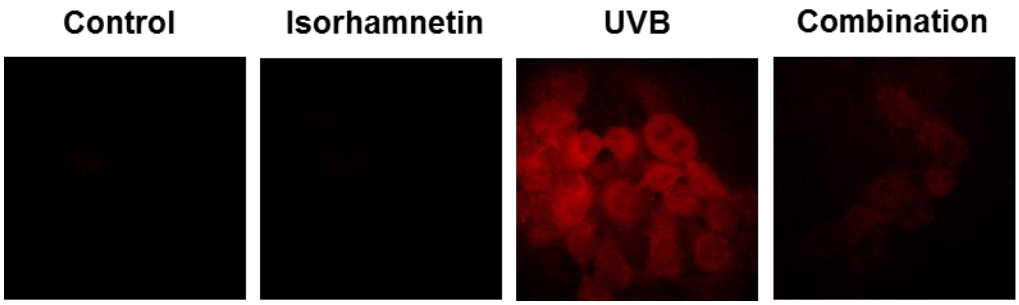

E

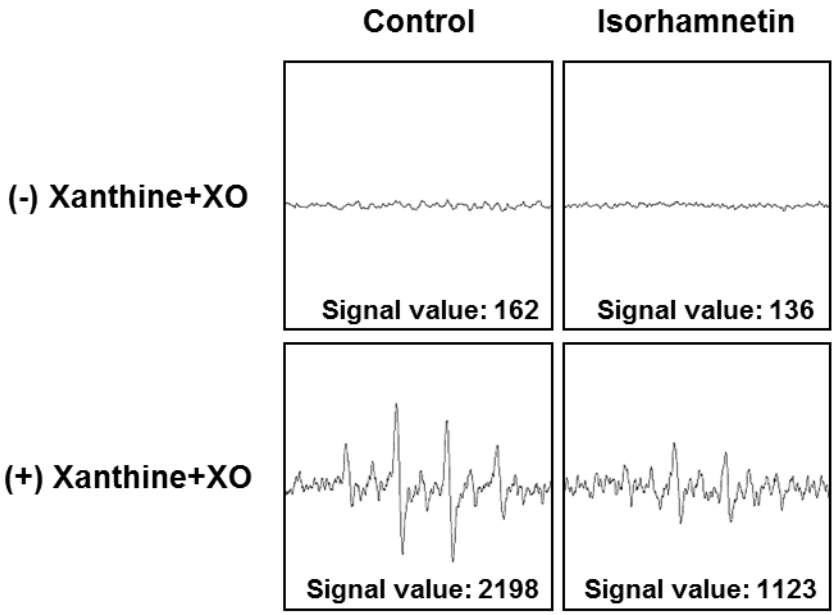

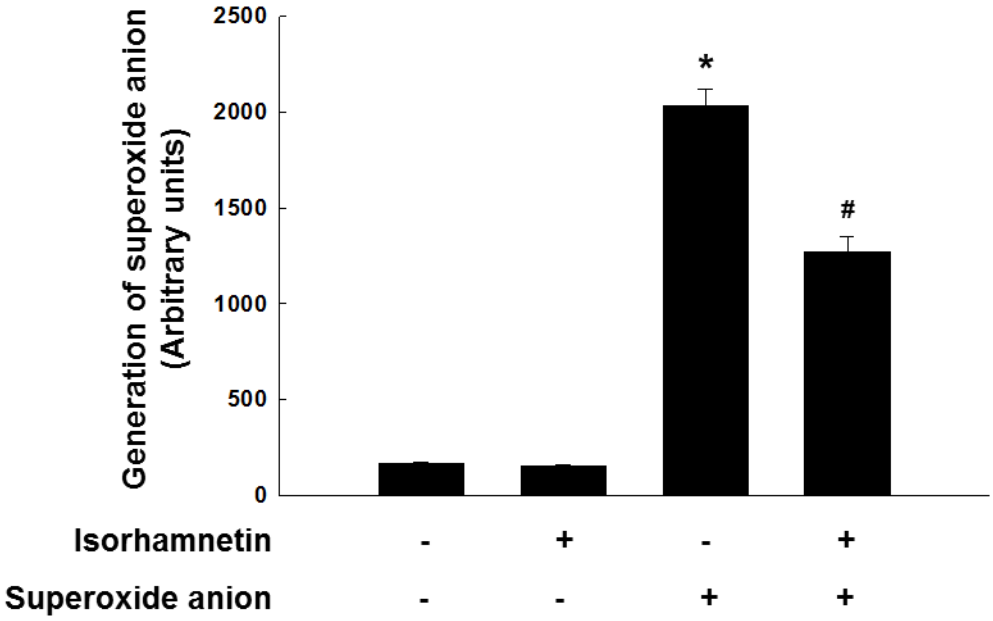

F

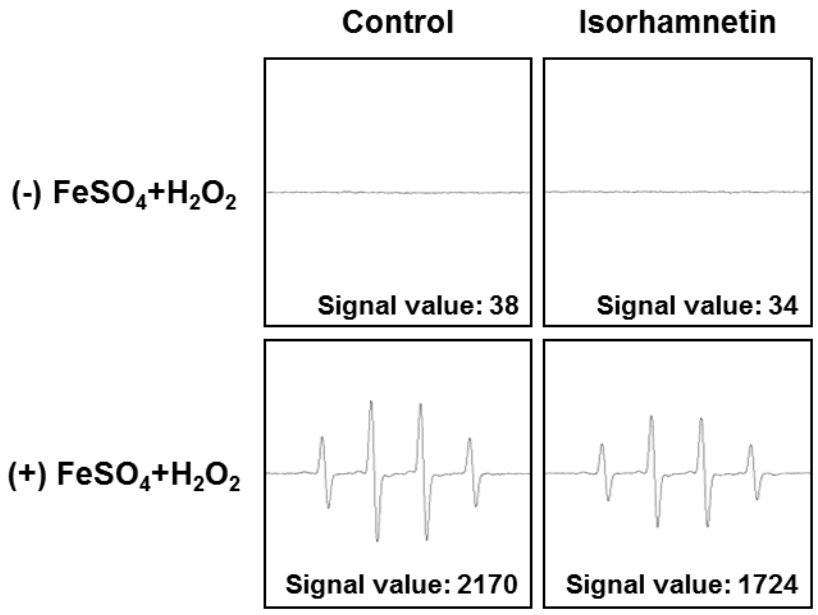

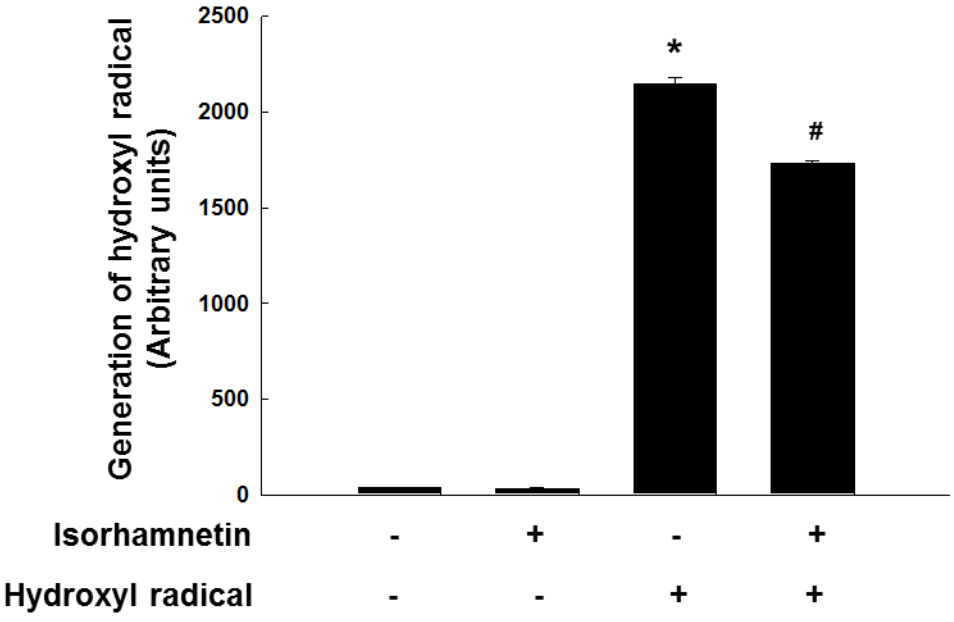

FIGURE 1. Isorhamnetin scavenges ROS. (A) HaCaT keratinocytes were pretreated with isorhamnetin at various concentrations. After incubation for 24 h, cell viability was assessed by the MTT assay. Cell viability is expressed in each case as a percentage of the untreated control (100%). Cells were treated with 5 μM isorhamnetin for 1 h (B–D) or 1 mM NAC for (B), and then exposed to UVB light. After incubation for 30 min, intracellular ROS levels were detected using (B) fluorescence spectrofluorometry, (C) flow cytometry, and (D) confocal microscopy after DCF-DA staining. [*]Significantly different from control ($p < 0.05$); [#]significantly different from UVB-irradiated cells ($p < 0.05$). FI: fluorescence intensity. Combination: isorhamnetin + UVB light. (E) The superoxide anion generated by the xanthine/xanthine oxidase (XO) system, and the resulting •OOH adducts were detected by ESR spectrometry. The results are expressed as representative peak data and histograms. Control: PBS; Isorhamnetin: isorhamnetin + PBS; Superoxide anion: PBS + xanthine + xanthine oxidase; Isorhamnetin + superoxide anion: isorhamnetin + xanthine + xanthine oxidase. (F) The hydroxyl radical generated by the Fenton reaction (H_2O_2 + $FeSO_4$) and the resulting •OH adducts were detected by ESR spectrometry. Results are expressed as representative peak data and histograms. Control: PBS; Isorhamnetin: isorhamnetin + PBS; Hydroxyl radical: PBS + $FeSO_4$ + H_2O_2; Isorhamnetin + hydroxyl radical: isorhamnetin + $FeSO_4$ + H_2O_2. [*]Significantly different from control ($p < 0.05$); [#]significantly different from UVB-irradiated cells ($p < 0.05$).

3-2. Isorhamnetin protects HaCaT keratinocytes against UVB-induced apoptosis

UVB radiation is well-known for its capacity to aggravate apoptosis in human keratinocytes (Schwarz *et al*., 1995). Therefore, the ability of isorhamnetin to improve cell survival in UVB-irradiated HaCaT keratinocytes was next investigated. Cell viability was significantly reduced in UVB-exposed vs. untreated control cells. Nevertheless, isorhamnetin pretreatment significantly overturned the effects of UVB light, with 81.13 vs. 68.80% cell viability observed in UVB-irradiated/isorhamnetin-pretreated vs. UVB-irradiated cultures (Fig. 2A).

Dynamic changes in nuclear chromatin compaction are characteristic of apoptotic execution (Wyllie *et al*., 1984). Therefore, cell nuclei were stained with Hoechst 33342 dye to measure nuclei condensation via fluorescence microscopy. Obvious nuclei condensation were occurred in UVB-irradiated cells (apoptotic index = 6.69), while the nuclei condensation rate was dramatically reduced by isorhamnetin pretreatment (apoptotic index = 3.04; compare with 2.66 for the positive control, NAC) (Fig. 2B).

The cytoprotective effects of isorhamnetin against UVB-triggered apoptosis were additionally confirmed by determining the fraction of the cell population with apoptotic sub-G1 DNA contents. The percentage of cells with apoptotic sub-G1 DNA contents increased from 3% and 2% in untreated control and isorhamnetin-pretreated cells, respectively, to 25% in UVB-irradiated cells. Nonetheless, isorhamnetin pretreatment significantly decreased this value to 12% (Fig. 2C). Moreover, the high level of DNA fragmentation in UVB-irradiated cells was significantly overturned by isorhamnetin pretreatment, as evidenced by the TUNEL assay (Fig. 2D).

A

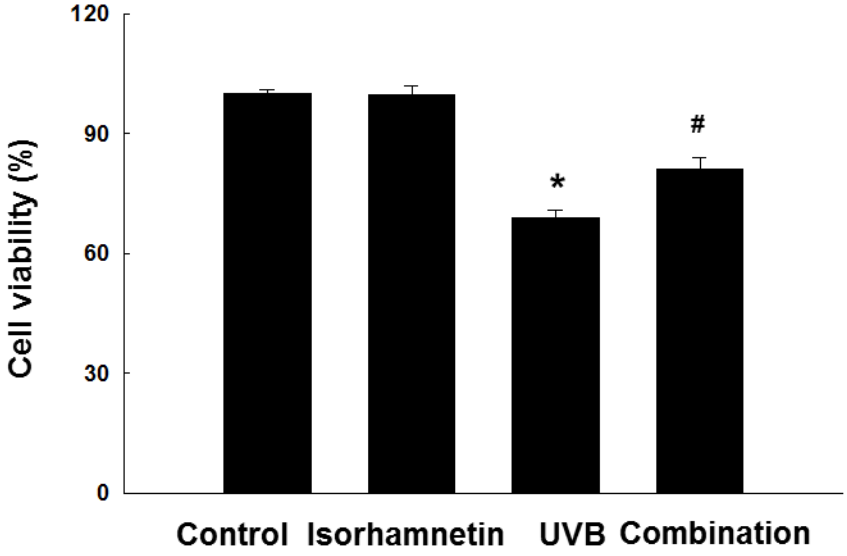

B

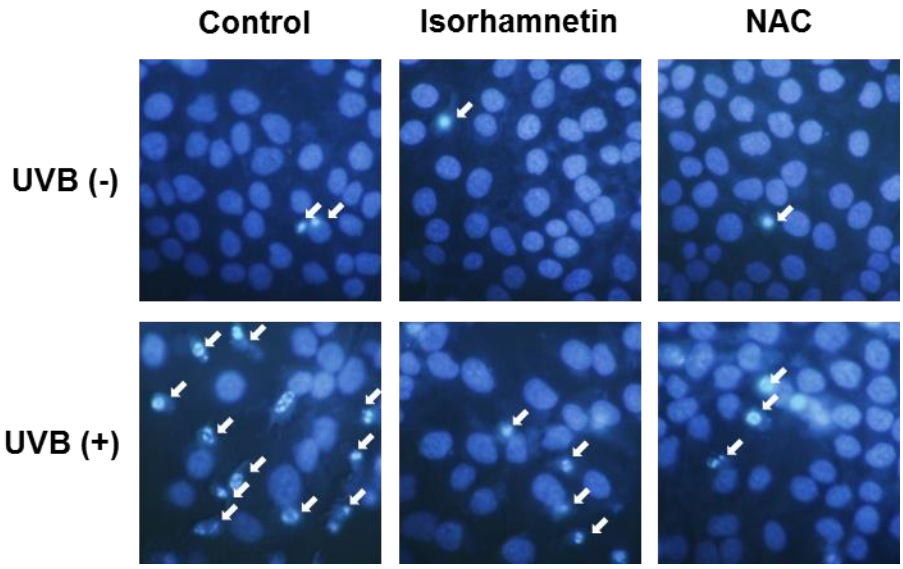

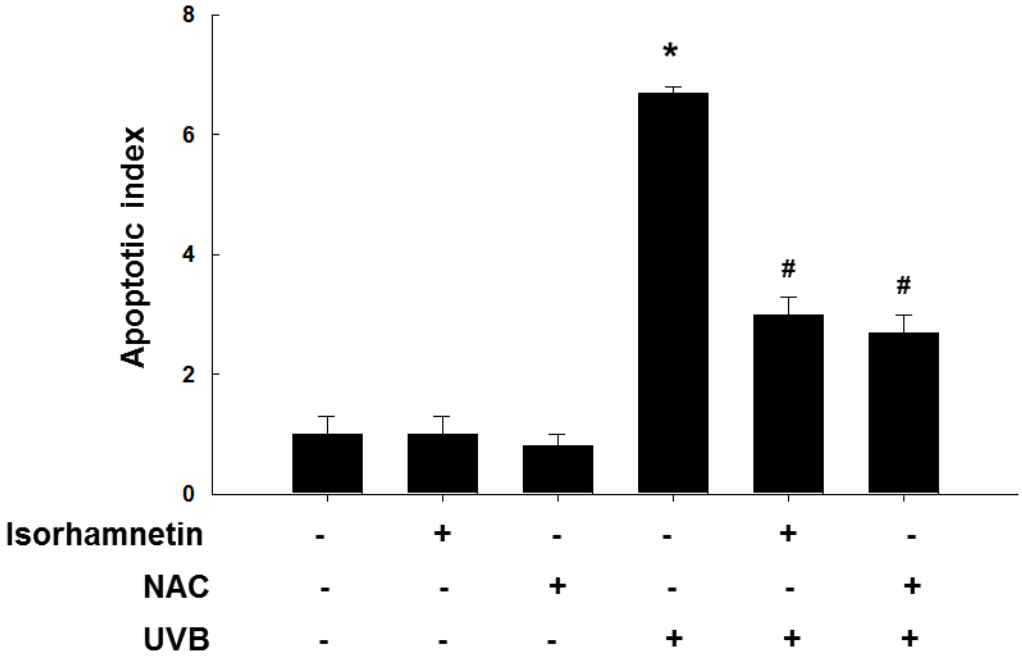

C

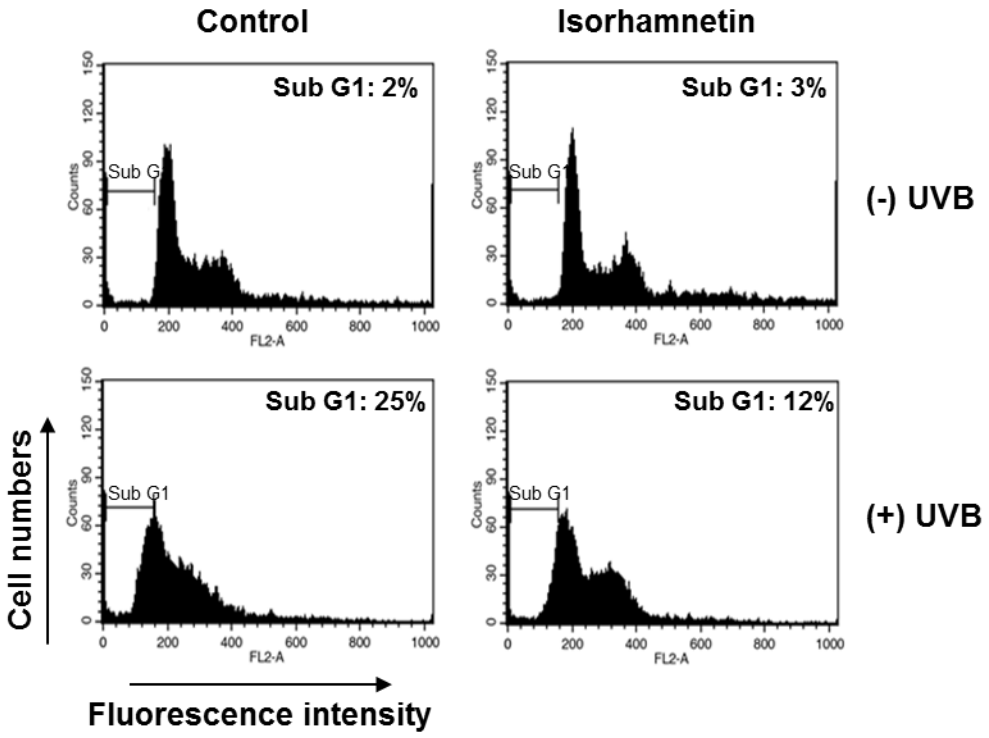

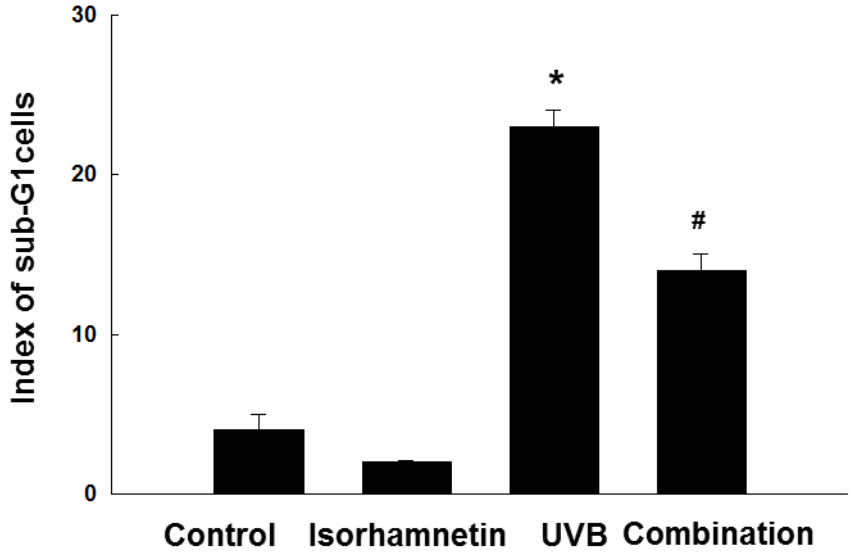

D

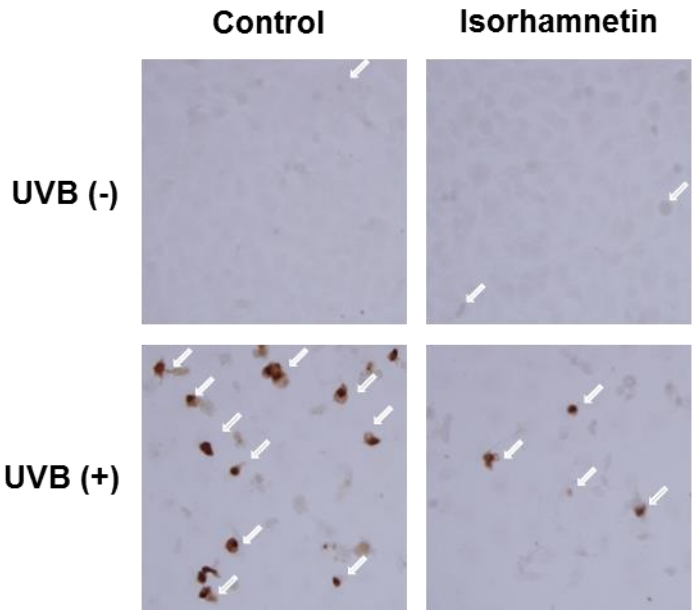

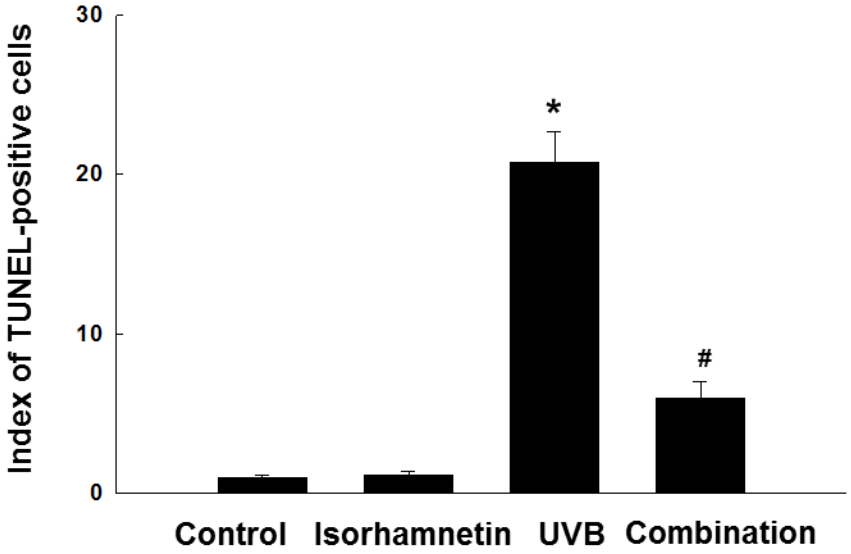

FIGURE 2. Isorhamnetin ameliorates UVB-induced apoptosis. (A) HaCaT keratinocytes were pretreated with 5 μM isorhamnetin, exposed to UVB light 1 h later, and incubated for another 24 h. Cell viability was then determined using the MTT assay. Cell viability is expressed in each case as a percentage of the untreated control (100%). (B) Cells were stained with Hoechst 33342 dye, and apoptotic bodies (arrows) were observed by fluorescence microscopy and quantitated. (C) Cells with apoptotic sub-G1 DNA contents were detected by flow cytometry after propidium iodide staining. (D) Apoptotic cells were detected by the TUNEL assay and quantitated. The arrows indicate TUNEL-positive cells. *Significantly different from control ($p < 0.05$); #significantly different from UVB-irradiated cells ($p < 0.05$). Combination: isorhamnetin + UVB light.

3-3. Isorhamnetin inhibits UVB-induced mitochondrial dysfunction

Apoptosis is mediated via mitochondrial membrane permeabilization/depolarization events (Landes and Martinou, 2011). Ample evidence demonstrates that UVB irradiation leads to a loss of mitochondrial membrane potential ($\Delta\psi_m$) (Mencucci *et al*., 2014; Kim *et al*., 2014). In order to investigate whether isorhamnetin can protect HaCaT cells from UVB-induced apoptosis stemming from mitochondrial dysfunction, the confocal microscopy and flow cytometry were employed to measure the fluorescence intensity of JC-1 dye. By using confocal microscopy analysis, the mitochondria of UVB-irradiated cells strongly fluoresced green, indicative of $\Delta\psi_m$ depolarization. However, the increased green fluorescence intensity triggered by UVB was nearly prevented by isorhamnetin pretreatment (Fig. 3A). The flow cytometry data showed coincident results (Fig. 3B), suggesting that isorhamnetin attenuates UVB-induced disruption of $\Delta\psi_m$ in HaCaT keratinocytes.

A

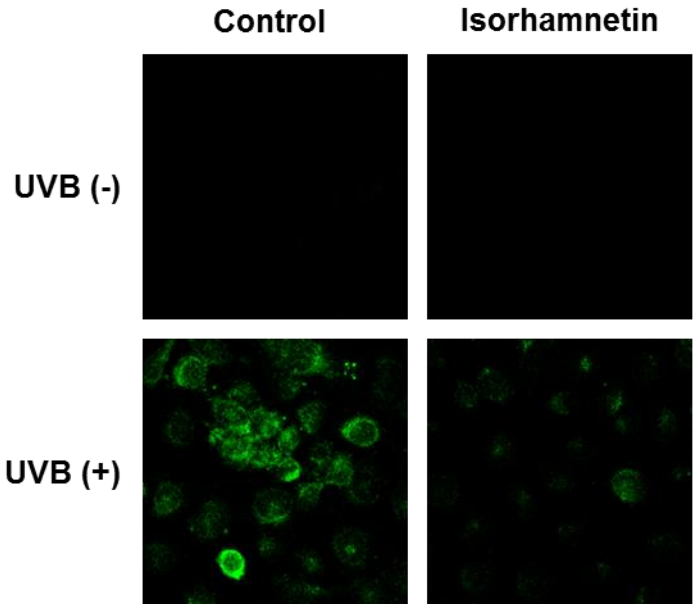

B

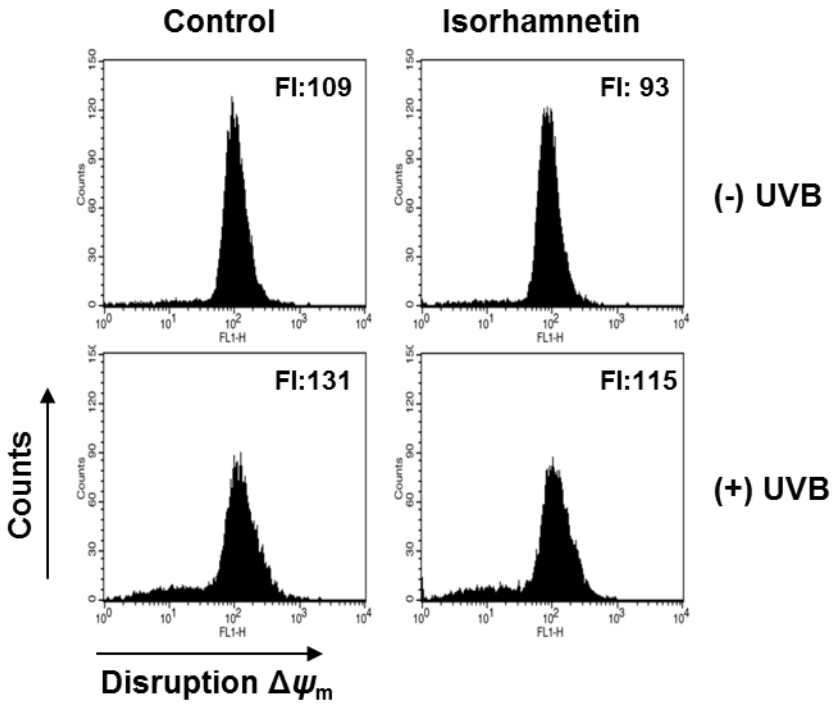

FIGURE 3. Isorhamnetin inhibits UVB-induced mitochondrial dysfunction. Isorhamnetin pretreatment impedes the loss of mitochondrial membrane potential in HaCaT keratinocytes after UVB exposure, as determined by (A) confocal microscopy and (B) flow cytometry of JC-1-stained cells. FI: fluorescence intensity.

3-4. Isorhamnetin protects HaCaT keratinocytes against UVB-facilitated macromolecular damage

Excessive UVB irradiation induced DNA strand breakage in keratinocytes was substantially visualized and assessed by the comet assay, where DNA tail length represents the degree of DNA lesion. The increasing values both were observed in comet tail length and the percentage of total cellular fluorescence in the comet tails in UVB-irradiated vs. untreated control keratinocytes, whereas isorhamnetin pretreatment significantly decreased (Fig. 4A).

UVB light can also causes oxidative damage to cellular lipids. The 8-isoprostane levels secreted into the conditioned medium by HaCaT keratinocytes were measured to assess Lipid peroxidation. UVB-exposed cells secreted higher level of 8-isoprostane relative to unexposed control cells, however pretreated with isorhamnetin obviously decreased contents of 8-isoprostane in irradiated cells, without having any effects of its own (Fig. 4B). The capability of isorhamnetin to rescue UVB-induced oxidative lipid injury was further confirmed by confocal microcopy of DPPP oxide fluorescence in DPPP-stained cells (Fig. 4C).

Finally, protein carbonylation is an indication of oxidative stress-induced damage to macromolecular proteins (Dalle-Donne *et al*., 2003). UVB exposure significantly up-regulated protein carbonyl contents in HaCaT keratinocytes, but this action was prevented by isorhamnetin pretreatment (Fig. 4D).

A

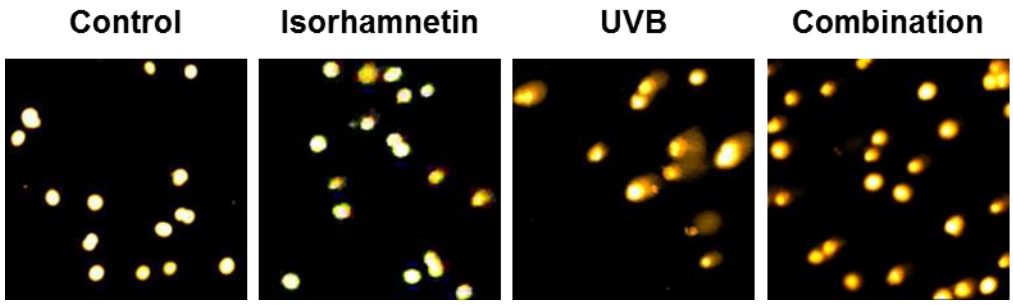

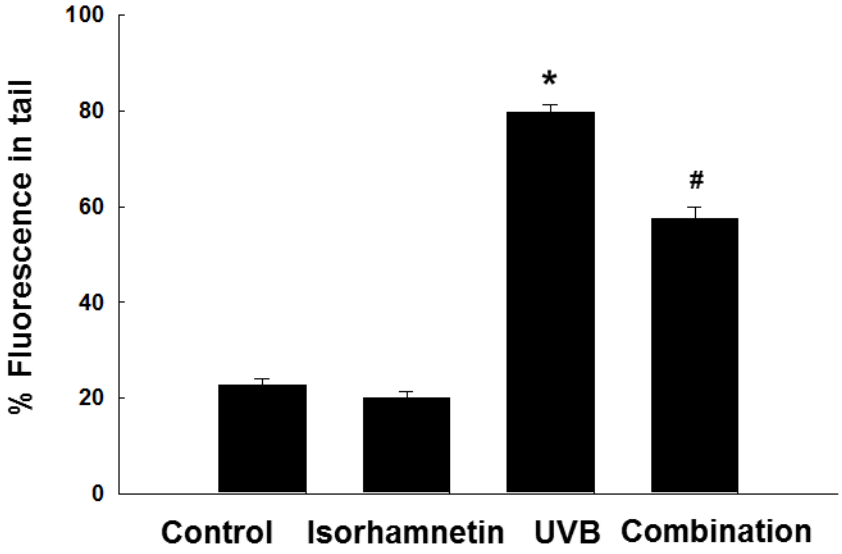

B

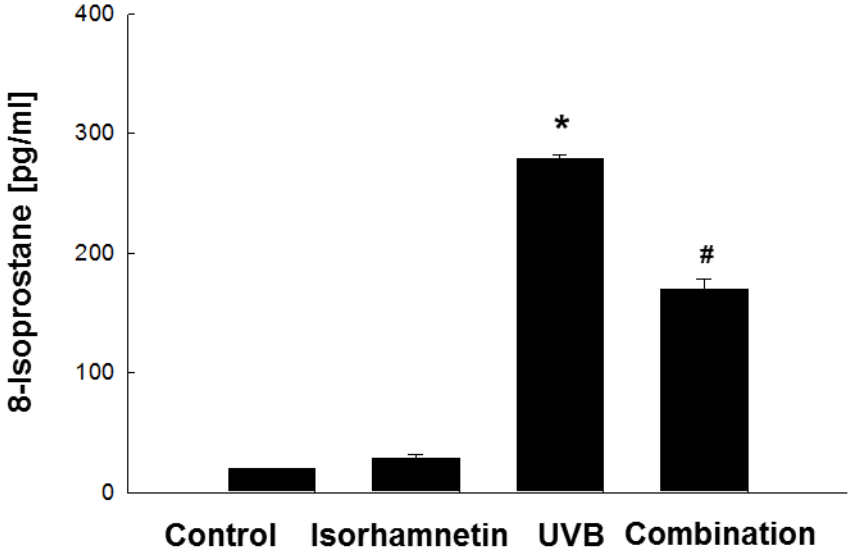

C

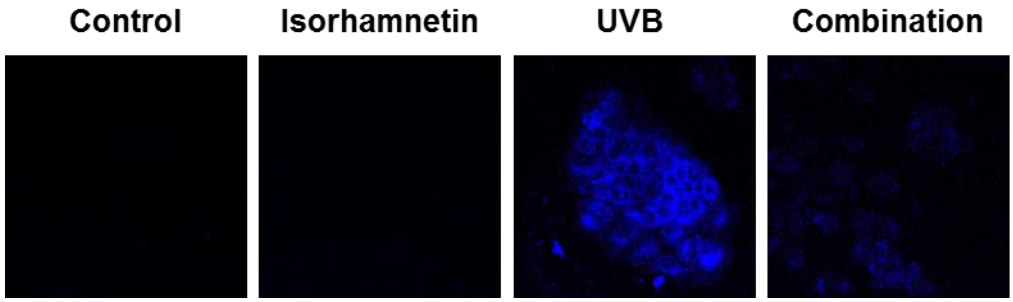

D

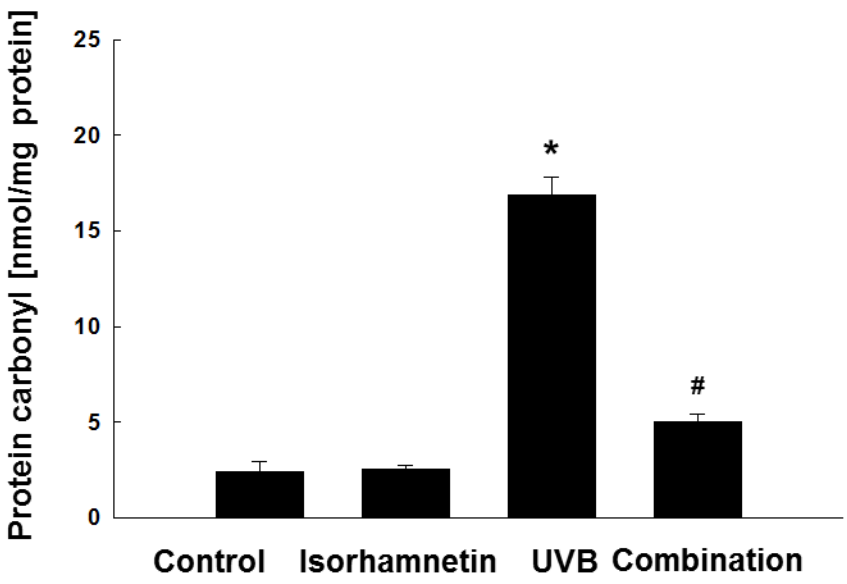

FIGURE 4. Isorhamnetin protects HaCaT keratinocytes against UVB-induced oxidative macromolecular damage. (A) DNA damage was detected by the comet assay. (B and C) lipid peroxidation was detected by (B) measurement of 8-isoprostane levels in the conditioned media and (C) detection of lipid hydroperoxides in DPPP-stained cells by fluorescence microscopy. (D) Protein oxidation was assayed by measurement of protein carbonyl levels. *Significantly different from control ($p < 0.05$); #significantly different from UVB-irradiated cells ($p < 0.05$). Combination: isorhamnetin + UVB light.

4. Discussion

Isorhamnetin is a naturally occurring, methylated flavonoid. The biological activities of isorhamnetin are reportedly greater than those of its unmethylated parent compound, which might due to the increased absorption and metabolic stability of methylated flavonoids (Wen and Walle, 2006). In the current study, the antioxidant and cytoprotective effects of isorhamnetin against UVB-induced damage in keratinocytes, the predominant cell type found in the human epidermis were investigated. The findings indicate that isorhamnetin has no cytotoxic at concentrations of ≤5 μM to keratinocytes (Fig. 1A), and may therefore find utility as part of a therapeutic arsenal against UVB-provoked skin damage.

Because of its special chemical structure features, the hydroxyl group is an indispensable functional group of many natural antioxidants, including isorhamnetin and other polyphenols (Sim *et al*., 2007). Since the reactive nature of ROS is own to their unpaired electrons, the phenolic hydroxyl group donation of a hydrogen atom acts to effectively quench ROS (Choi *et al*., 2002; Heim *et al*., 2002; Valentão *et al*., 2003). Consistent with these reports, the present results revealed that isorhamnetin efficiently scavenged intracellular ROS in HaCaT keratinocytes (Fig. 1B–D), and also directly quenched the superoxide anion and the hydroxyl radical in cell-free systems (Fig. 1E and F). Therefore, the ROS scavenging ability of isorhamnetin may be due to the three phenolic hydroxyl groups in its structure.

UVB-induced apoptosis is mediated by a number of molecular processes, which target the mitochondria and activate the mitochondria-initiated cell death pathway (Ji *et al*., 2014). These processes include changes in the $\Delta\psi_m$, production of intracellular ROS, opening of the mitochondrial permeability transition pore, and release of cytochrome c from the mitochondrion into the cytoplasm. Consequently, mitochondria rapidly lose their transmembrane potential during apoptosis, generating excessive amounts of intracellular ROS (Ricci *et al*., 2003) and attenuating cell viability. In addition to substantially protecting human keratinocytes from UVB-provoked programmed cell death and mitochondrial dysfunction (Figs. 2 and 3), isorhamnetin also rescued cell viability in UVB-exposed HaCaT

keratinocytes (Fig. 2).

Abnormal production of ROS leads to oxidative damage to macromolecules, including DNA, lipids, and proteins (Ray *et al*., 2012; Pashikanti *et al*., 2011), which contributes to considerable disruption of normal cellular functions. Notably, the present study showed that isorhamnetin pretreatment attenuated UVB-exposure levels of DNA strand breakage, protein carbonyl formation, and lipid peroxidation in HaCaT keratinocytes (Fig. 4).

In conclusion, the results of this study demonstrate that isorhamnetin suppresses the deleterious effects of UVB irradiation in human keratinocytes, including excessive intracellular ROS generation, oxidative damage to DNA, lipids, and proteins, and mitochondrial dysfunction. Moreover, isorhamnetin improves cell viability and inhibits apoptosis in UVB-exposed human keratinocytes. These data support the hypothesis that isorhamnetin might be utilized as a novel antioxidant agent to treat ROS-related skin disorders. Nevertheless, the biological efficacy of isorhamnetin in vivo and the underlying mechanisms of isorhamnetin action require further exploration.

All the main contents and experimental data are derived from the paper of "*Isorhamnetin Protects Human Keratinocytes against Ultraviolet B-Induced Cell Damage*", which has been published in the journal as "*DOI: 10.4062/biomolther.2015.005, Biomolecules & therapeutics, Jul 2015*".

5. References

Afaq, F. (2011) Natural agents: cellular and molecular mechanisms of photoprotection. *Arch. Biochem. Biophys.* 508, 144-151.

Beauchamp, M. C. and Letendre, E. and Renier, G. (2002) Macrophage lipoprotein lipase expression is increased in patients with heterozygous familial hypercholester-olemia. *J. Lipid Res.* 43, 215-222.

Budden, T. and Bowden, N. A. (2013) The role of altered nucleotide excision repair and UVB-induced DNA damage in melanomagenesis. *Int. J. Mol. Sci.* 14, 1132-1151.

Carmichael, J., DeGraff, W. G., Gazdar, A. F., Minna, J. D. and Mitchell, J. B. (1987) Evaluation of a tetrazolium-based semiautomated colorimetric assay: assessment of chemosensitivity testing. *Cancer Res.* 47, 936-942.

Choi, H. R., Choi, J. S., Han, Y. N., Bae, S. J. and Chung, H. Y. (2002) Peroxynitrite scavenging activity of herb extracts. *Phytother. Res.* 16, 364-367.

Cossarizza, A., Baccarani-Contri, M., Kalashnikova, G. and Franceschi, C. (1993) A new method for the cytofluorimetric analysis of mitochondrial membrane potential using the J-aggregate forming lipophilic cation 5,5 ′,6,6 ′-tetrachloro-1,1 ′,3,3 ′-tetraethylbenzimidazolcarbocyanine iodide (JC-1). *Biochem. Biophys. Res. Commun.* 197, 40-45.

Dalle-Donne, I., Rossi, R., Giustarini, D., Milzani, A. and Colombo, R. (2003) Protein carbonyl groups as biomarkers of oxidative stress. *Clin. Chim. Acta.* 329, 23-38.

Everett, M. A., Yeargers, E., Sayre, R. M. and Olson R. L. (1966) Penetration of epidermis by ultraviolet rays. *Photochem. Photobiol.* 5, 533-542.

Heim, K. E., Tagliaferro, A. R. and Bobilya, D. J. (2002) Flavonoid antioxidants: chemistry, metabolism

and structure-activity relationships. *J. Nutr. Biochem.* 13, 572-584.

Helenius, M., Makelainen, L. and Salminen A. (1999) Attenuation of NF-kappaB signaling response to UVB light during cellular senescence. *Exp. Cell Res.* 248, 194-202.

Ji, Y., Cai, L., Zheng, T., Ye, H., Rong, X., Rao, J. and Lu, Y. (2014) The mechanism of UVB irradiation induced-apoptosis in cataract. *Mol. Cell Biochem.* 401, 87-95.

Kim, K. C., Piao, M. J., Zheng, J., Yao, C. W., Cha, J. W., Kumara, M. H., Han, X., Kang, H. K., Lee, N. H. and Hyun, J. W. (2014) Fucodiphlorethol G purified from ecklonia cava suppresses ultraviolet B radiation-induced oxidative stress and cellular damage. *Biomol. Ther.* 22, 301-307.

Kohno, M., Mizuta, Y., Kusai, M., Masumizu, T. and Makino, K. (1994) Measurements of superoxide anion radical and superoxide anion scavenging activity by electron spin resonance spectroscopy coupled with DMPO spin trapping. *Bull. Chem. Soc. Jpn.* 67, 1085-1090.

Landes, T. and Martinou, J. C. (2011) Mitochondrial outer membrane permeabilization during apoptosis: the role of mitochondrial fission. *Biochim. Biophys. Acta*. 1813, 540-545.

Lee, C. W., Ko, H. H., Chai, C. Y., Chen, W. T., Lin, C. C. and Yen, F. L. (2013) Effect of *Artocarpus communis* extract on UVB irradiation-induced oxidative stress and inflammation in hairless mice. *Int. J. Mol. Sci.* 14, 3860-3873.

Li, C., Yang, X., Chen, C., Cai, S. and Hu, J. (2014) Isorhamnetin suppresses colon cancer cell growth through the PI3K-Akt-mTOR pathway. *Mol. Med. Rep.* 9, 935-940.

Li, L., Abe, Y., Mashino, T., Mochizuki, M. and Miyata, N. (2003) Signal enhancement in ESR spin-trapping for hydroxyl radicals. *Anal. Sci.* 19, 1083-1084.

Liu, S., Guo, C., Wu, D., Ren, Y., Sun, M. Z. and Xu, P. (2012) Protein indicators for HaCaT cell damage

induced by UVB irradiation. *J. Photochem. Photobiol. B* 114, 94-101.

Lyu, S. Y. and Park, W. B. (2012) Photoprotective potential of anthocyanins isolated from *Acanthopanax divaricatus* Var. albeofructus fruits against UV irradiation in human dermal fibroblast cells. *Biomol. Ther.* 20, 201-206.

Matsumura, Y. and Ananthaswamy, H. N. (2004) Toxic effects of ultraviolet radiation on the skin. *Toxicol. Appl. Pharmacol.* 195, 298-308.

Mencucci, R., Favuzza, E., Boccalini, C., Lapucci, A., Felici, R., Resta, F., Chiarugi, A. and Cavone, L. (2014) CoQ10-containing eye drops prevent UVB-induced cornea cell damage and increase cornea wound healing by preserving mitochondrial function. *Invest. Ophthalmol. Vis. Sci.* 55, 7266-7271.

Okimoto, Y., Watanabe, A., Niki, E., Yamashita, T. and Noguchi, N. (2000) A novel fluorescent probe diphenyl-1-pyrenylphosphine to follow lipid peroxidation in cell membranes. *FEBS Lett.* 474, 137-140.

Pashikanti, S., Boissonneault, G. A. and Cervantes-Laurean, D. (2011) Ex vivo detection of histone H1 modified with advanced glycation end products. *Free Radic. Biol. Med.* 50, 1410-1416.

Rajagopalan, R., Ranjan, S. and Nair, C. K. (2003) Effect of vinblastine sulfate on gamma-radiation-induced DNA single-strand breaks in murine tissues. *Mutat. Res.* 536, 15-25.

Ray, P. D., Huang, B. W. and Tsuji, Y. (2012) Reactive oxygen species (ROS) homeostasis and redox regulation in cellular signaling. *Cell Signal* 24, 981-990.

Ricci, J. E, Gottlieb, R. A. and Green, D. R. (2003) Caspase-mediated loss of mitochondrial function and generation of reactive oxygen species during apoptosis. *J. Cell Biol.* 160, 65-75.

Rosenkranz, A. R., Schmaldienst, S., Stuhlmeier, K. M., Chen, W., Knapp, W. and Zlabinger, G. J. (1992) A microplate assay for the detection of oxidative products using 2′,7′-dichlorofluorescin-diacetate. *J.*

Immunol. Methods 156, 39-45.

Rosette, C. and Karin, M. (1996) Ultraviolet light and osmotic stress: activation of the JNK cascade through multiple growth factor and cytokine receptors. *Science* 274, 1194-1197.

Sander, C. S., Chang, H., Hamm, F., Elsner, P. and Thiele, J. J. (2004) Role of oxidative stress and the antioxidant network in cutaneous carcinogenesis. *Int. J. Dermatol.* 43, 326-335.

Scandalios, J. G. (2002) The rise of ROS. *Trends Biochem. Sci.* 27, 483-486.

Schwarz, A., Bhardwaj, R., Aragane, Y., Mahnke, K., Riemann, H., Metze, D., Luger, T. A. and Schwarz, T. (1995) Ultraviolet-B-induced apoptosis of keratinocytes: evidence for partial involvement of tumor necrosis factor-α in the formation of sunburn cells. *J. Invest. Dermatol.* 104, 922-927.

Sim, G. S., Lee, B. C., Cho, H. S., Lee, J. W., Kim, J. H., Lee, D. H., Kim, J. H., Pyo, H. B., Moon, D. C., Oh, K. W., Yun, Y. P. and Hong, J. T. (2007) Structure activity relationship of antioxidative property of flavonoids and inhibitory effect on matrix metalloproteinase activity in UVA-irradiated human dermal fibroblast. *Arch. Pharm. Res.* 30, 290-298.

Singh, N. P. (2000) Microgels for estimation of DNA strand breaks, DNA protein crosslinks and apoptosis. *Mutat. Res.* 455, 111-127.

Ueno, I., Kohno, M., Yoshihira, K. and Hirono, I. (1984) Quantitative determination of the superoxide radicals in the xanthine oxidase reaction by measurement of the electron spin resonance signal of the superoxide radical spin adduct of 5,5-dimethyl-1-pyrroline-1-oxide. *J. Pharmacobiodyn.*7, 563-569.

Valentão, P., Fernandes, E., Carvalho, F., Andrade, P. B., Seabra, R. M. and Bastos, M. L. (2003) Hydroxyl radical and hypochlorous acid scavenging activity of small centaury (*Centaurium erythraea*) infusion. A comparative study with green tea (*Camellia sinensis*). *Phytomedicine* 10, 517-522.

W äster, P. K. and Ollinger, K. M. (2009) Redox-dependent translocation of p53 to mitochondria or nucleus in human melanocytes after UVA- and UVB-induced apoptosis. *J. Invest. Dermatol.* 129, 1769-1781.

Wen, X. and Walle, T. (2006) Methylated flavonoids have greatly improved intestinal absorption and metabolic stability. *Drug Metab. Dispos.* 34, 1786-1792.

Wyllie, A., Morris, R., Smith, A. and Dunlop, D. (1984) Chromatin cleavage in apoptosis: association with condensed chromatin morphology and dependence on macromolecular synthesis. *J. Pathol.* 142, 67-77.

Yang, J. H., Shin, B. Y., Han, J. Y., Kim, M. G., Wi, J. E., Kim, Y. W., Cho, I. J., Kim, S. C., Shin, S. M. and Ki, S. H. (2014) Isorhamnetin protects against oxidative stress by activating Nrf2 and inducing the expression of its target genes. *Toxicol. Appl. Pharmacol.* 274, 293-301.

Yin, Y., Li, W., Son, Y. O., Sun, L., Lu, J., Kim, D., Wang, X., Yao, H., Wang, L., Pratheeshkumar, P., Hitron, A. J., Luo, J., Gao, N., Shi, X. and Zhang, Z. (2013) Quercitrin protects skin from UVB-induced oxidative damage. *Toxicol. Appl. Pharmacol.* 269, 89-99.

Zeng, J. P., Bi, B., Chen, L., Yang, P., Guo, Y., Zhou, Y. Q. and Liu, T. Y. (2014) Repeated exposure of mouse dermal fibroblasts at a sub-cytotoxic dose of UVB leads to premature senescence: a robust model of cellular photoaging. J. Dermatol. Sci. 73, 49-56.

6. Abstract in Korean

본 연구의 목적은 인간 HaCaT 각질형성세포에서 자외선(UV) B의 노출로 인한 세포손상에 대하여 특정 약용 식물에서 분리된 플라보노이드, isorhamnetin (3-methylquercetin)의 광 보호 특성을 밝히는 것이다. Isorhamnetin은 인간 HaCaT 각질형성세포에서 UVB로 생성된 세포 내 활성산소종의 소거능을 나타내었고 UVB로 유도되는 자멸소체(apoptotic body)의 형성, 핵 분절화(nuclear fragmentation) 및 아포토틱 sub-G1 DNA 파편을 확연하게 감소시킴으로써 세포자멸사를 억제하였다. 또한, Isorhamnetin은 UVB 노출에 의한 지질, 단백질 및 DNA와 같은 거대분자의 산화손상을 감소시켰다. 이 외에도 isorhamnetin은 UVB로 유도된 미토콘드리아 기능장애로부터 HaCaT 각질형성세포를 보호하였다. 이러한 결과는 isorhamnetin이 UVB로 매개되는 피부 질환에 대한 효율적인 제제로 개발될 수 있는 특수성을 가지고 있음을 암시한다.

7. Acknowladgements

I would like deeply show my sincere gratitude to my direct supervisor Prof. Jin-Won Hyun, who gave me a lot of encouragement and guidance during my master degree period in Jeju National University, Republic of Korea. In the past two years, her serious-minded academic attitude on research and the rigorous way of thinking would carry me through the end of my research career.

I greatly appreciate to Prof. Deok-Bae Park and Prof. Hee-Kyoung Kang, School of Medicine in Jeju National University, who supervised a lot in my thesis to complete my master graduate dissertation. Additionally, all other professors for providing knowledge of biochemical techniques and training me the capability of analysis are also greatly thankful.

My particularly appreciate is to my lab members, especially the tutor of Ph.D. Mei-Jing Piao for her keen attention, patience and experimental suggestions throughout my study. I would also like to thank my seniors Dr. Ki-Cheon Kim, Cheng-Wen Yao, Jian Zheng, and Ji-Won Cha, and my colleague and friends of Susara Ruwan Kumara Madduma Hewage, Min-Chang Oh, Pattage Madushan Dilhara Jayatissa Fernando for supporting me all the time in my daily life and also on my experiments.

Finally, I would to show my great feeling of gratitude to my parents who always stand by me. Their empathetic listening, kind understanding and unconditional supporting have been risen me up all the time.